Int. J. Solids Structures Vol. 15, pp. 669–683

0020-7683/79/0901-0669/$02.00/0

AN EXPERIMENTAL STUDY OF THE PLASTIC BUCKLING OF CIRCULAR CYLINDERS IN PURE BENDING

B. D. REDDY†
Department of Civil and Municipal Engineering, University College London, Gower Street, London WCIE 6BT, England‡

(*Received* 31 *May* 1978; *in revised form* 29 *August* 1978)

Abstract—An experimental investigation into the plastic buckling of cylindrical tubes subjected to bending moments at the ends is reported on. Suitable parameters by means of which the buckling moment may be represented are first discussed, and after a description of the apparatus and the testing procedure, the results of tests on stainless steel and aluminium alloy tubes are given. These results are compared with analytical results for the collapse of cylinders under pure bending, and uniform axial compression. The mode of deformation of the cylinders is discussed and the experimental strains are compared with those of others for tests on axially compressed cylinders as well as cylinders in pure bending. The strains lie within ±30% of those predicted by J_2 deformation theory for cylinders in axial compression: the corresponding range of stresses is about ±5%.

NOTATION

E	Young's modulus
E_S	secant modulus
E_T	tangent modulus
k	dimensionless curvature, $= \kappa r^2/t$
M	bending moment
m	dimensionless moment, $= M/E\pi rt^2$
n	exponent in stress–strain relations, eqn (1)
r	mean radius
t	wall thickness
z	change in diameter/original diameter
ϵ	uniaxial strain
ϵ_{exp}	maximum extreme fibre compressive strain
ϵ_{ce}	classical buckling strain of elastic axially compressed cylinder
ϵ_{ci}	buckling strain of elastic–plastic axially compressed cylinder, from J_2 flow theory
ϵ_{cd}	buckling strain of elastic–plastic axially compressed cylinder, from J_2 deformation theory
κ	Longidudinal curvature
λ_{exp}	experimental value of average axial half-wavelength
λ_d	axial half-wavelength corresponding to ϵ_{cd}
λ_i	axial half-wavelength corresponding to ϵ_{ci}
σ	uniaxial stress
σ_R	stress in Ramberg–Osgood relation, eqn (1)
σ_{cd}	buckling stress of elastic plastic, axially compressed cylinder, from J_2 deformation theory
σ_{ci}	buckling stress of elastic plastic, axially compressed cylinder, from J_2 flow theory

INTRODUCTION

In any practical process of laying or manipulating submarine pipelines, it is not possible to avoid bending the pipe. Now if any initially straight thin-walled tube is bent far enough it will buckle, and form a kink. This may be demonstrated on any convenient tubing, e.g. a drinking straw. It is important to avoid the formation of such buckles in submarine pipelines, since it is costly to retrieve and replace any section of pipe, and moreover a buckle, once formed, may propagate as a flattening of the pipe for an indefinite distance under moderate hydrostatic pressure[1].

It is therefore desirable for pipeline engineers to know reasonably closely under what circumstances a thin-walled tube will buckle when it is subjected to pure bending, as well as to bending in the presence of external hydrostatic pressure.

Two modes of deformation manifest themselves in the buckling of uniform cylindrical shells acted upon by moments at their extreme ends. First, there is the Brazier effect[2] which

†Associate Research Assistant,
‡Present address: Department of Civil Engineering, Univ. of Cape Town, Rondebosch 7700, South Africa.

involves an increasing ovalisation of the cylindrical cross section with increase in moment, with the result that the moment-curvature relationship is nonlinear; and the moment eventually reaches a maximum or limit-point value. Secondly, the analytical treatment of the problem as a bifurcation buckling problem (with a linear membrane prebuckling state of stress) results in an eigenmode of the short-axial wave type. That is, axial waves form along the length of the cylinder, having a maximum amplitude at the extreme compression side of the shell and gradually diminishing around the circumference. This problem has been treated for the linear-elastic case by Seide and Weingarten[3] and by Reddy and Calladine[4]. In a real situation, it must be expected that both of these effects will be present simultaneously with one or the other dominating, depending on the proportions of the tube and the distribution of initial imperfections. Furthermore, the effects of plasticity will be present in metal tubes having a radius/thickness ratio of less than, say, 60.

Various workers [5–7] have performed experiments on specimens at various scales in order to establish the appropriate buckling criterion for pipes under pure bending. Submarine pipelines are usually made from steel tubing having a ratio of radius (r) to thickness (t) in the region of 30, and buckling takes place when much of the material is in the plastic range: only if the value of r/t were at least an order of magnitude higher would buckling occur in the elastic range. Now the tensile/compressive stress–strain curve for any ductile metal such as steel or aluminium alloy under steadily rising stress displays a more or less sharply curved "knee" when the plastic range is entered (see Fig. 1a), with the slope of the curve falling rapidly with increasing strain from the value (i.e. Young's modulus) corresponding to the initial, elastic portion. It follows that in the absence of buckling the bending moment-curvature relation for the pipe will have a broadly similar form (see Fig. 1b) and so, if buckling occurs in the plastic range it will do so at a bending moment which differs by relatively little from the " full plastic moment" of the tube. As Palmer[1] has pointed out, this unifying fact is of little practical value to engineers, since a detailed analysis is required to deduce the bending moments at any given section of a pipe during, e.g. the laying process. It is far easier to estimate the local radius of curvature of a pipe in the process of laying, from geometrical considerations. It is of course possible to transform a buckling criterion expressed in terms of bending moment into one expressed in terms of curvature, by using the curve of Fig. 1(b); and it is clear from the shape of this curve that even if buckling occurs over a relatively narrow range of bending moments, the criterion may, nevertheless, involve a relatively wide range of curvature. It

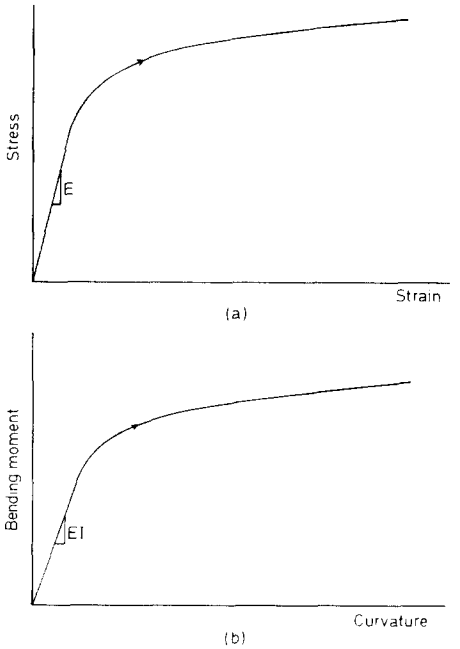

Fig. 1. (a) Typical uniaxial stress–strain curve for a strain-hardening metal; (b) moment-curvature curve for a tube in pure bending which has a stress–strain curve of the form shown in (a).

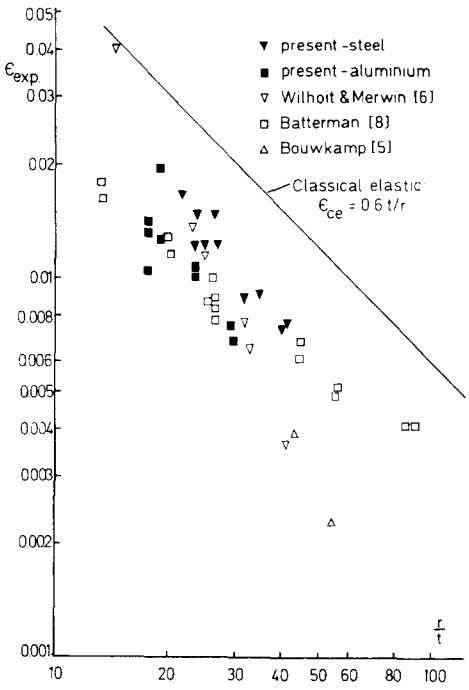

Fig. 2. Experimental values of critical extreme fibre compressive strain for tubes in bending, and critical strains for tubes in axial compression, vs r/t.

follows that *curvature* is a much more satisfactory measure of buckling processes than *bending moment*, or equivalently, that "*extreme fibre compressive strain*" is a better measure than the corresponding stress.

Palmer[1] has correlated the available experimental data on a logarithmic plot of "extreme fibre compressive strain" against the geometrical parameter r/t, as shown in Fig. 2: the open points refer to previous investigations and the solid ones to the results of our investigations, to be described later. Also shown in the figure are the points corresponding to values of buckling stress obtained by Batterman[8] in his experiments on the buckling of cylindrical shells in axial compression: the values of strain which we have plotted were found using Batterman's published results of buckling *stress* and the uniaxial stress–strain curve for his material, viz. aluminium alloy. Very broadly, the experimental observations over the range $13 < r/t < 50$ lie in a relatively narrow band of slope ~ -1.5. Also shown is the simple formula which comes from a classical elastic analysis[3, 4]. The data plotted in Fig. 2 were obtained from tests on tubes made from a range of materials having a wide range of stress–strain curves: but, unfortunately, in most cases details of the material behaviour are not reported.

The present investigation was undertaken with a view both to obtaining more data of the kind shown in Fig. 2; and also to elucidating the buckling process. Accordingly it was decided to test a series of tubes over a relatively wide range of ratios r/t in each of the different materials having rising stress–strain curves which had "sharp" and "rounded" knees, respectively. After some deliberation it was decided to standardise on tubes of 25 mm (1 in.) nominal diameter and approx. 600 mm (24 in.) long over the test section; and to use aluminium alloy and stainless steel for the two materials. Tubes were available in several thicknesses in each of the two materials, and it was possible to obtain a more finely graded range of thicknesses by means of a drawing process which was performed by UKAEA Reactor Fuel Laboratories.

DESCRIPTION OF APPARATUS

Figures 3(a) and 3(b) show two views of the apparatus used to carry out tests, while Fig. 4 shows a view of a typical test specimen and its end connections. In Fig. 4, the ends of the specimen (1) fit into collars (2) which are split in order to facilitate their assembly and removal. The bottom half of each collar fits snugly into the semi-circular recess machined out of the bottom half of the end block (3). The ends of the specimen are held in position by the top

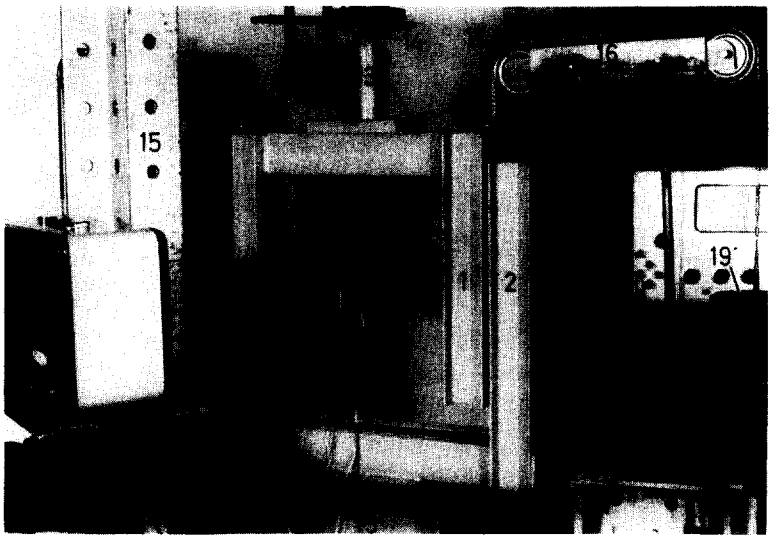

(a)

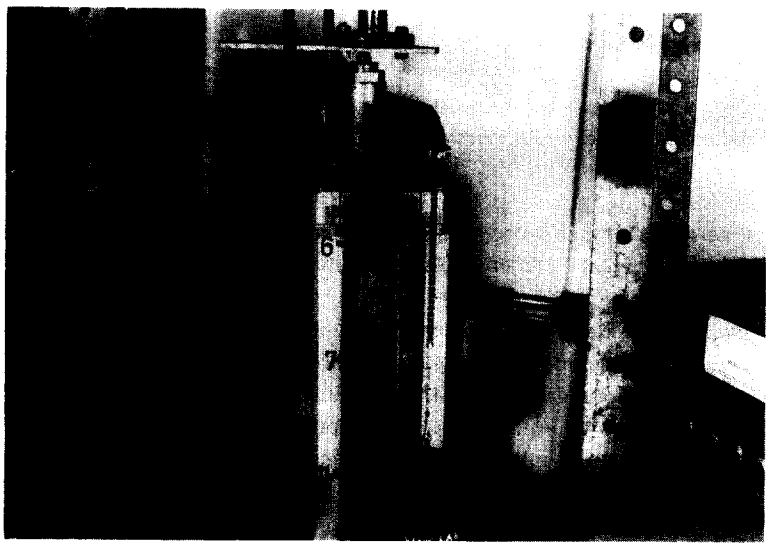

(b)

Figs. 3(a), (b). Views of apparatus used to carry out bending tests.

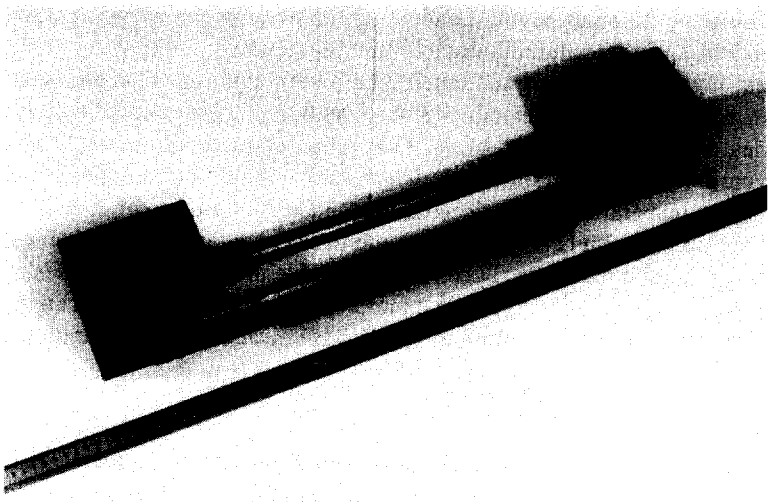

Fig. 4. Typical test specimen with end connections.

blocks (4) which hold the upper halves of the collars; these blocks are fastened down tightly on the bottom blocks by means of capscrews. The bar (5) is attached to the end blocks by means of hexagonal nuts which hold it down against the sides of the blocks. The blocks have dowels protruding from their sides, and the bar has a hole at one end and a slot (6) at the other. Spring washers are used between the nuts and the bar, so that the end blocks may rotate relatively freely, while the slot (6) ensures that the specimen may deform into an arc without restraint against longitudinal movement. The bar prevents any rotation about a longitudinal axis of the specimen.

Figures 3(a) and 3(b) show a typical test specimen (4) in position at the beginning of a test. The inner (1) and outer (2) frames are fabricated from channel sections, and the outer frame rests on a solid base (3). The arrangement is symmetrical with respect to the vertical planes passing through the longitudinal axis, and centre cross section of the specimen. The test specimen is supported at its extreme ends by strips of spring steel (5), which are bolted to the outer frame at (6) and to the extreme ends of the specimen end blocks at (7). Pairs of spring steel strips (8) are bolted to the specimen end connections at the points where the collars (9) enter the end blocks (10). The far ends of these strips are bolted to the inner frame at (11). A pure (i.e. without shear) bending moment is applied to the specimen by four-point loading, which is achieved by the downward displacement of the inner frame. The flexibility of the spring steel strips ensures that they offer negligible restraint against rotation at the ends. Nevertheless, the restraining moments induced in the strips were accounted for when calculating the applied moments, by calculations which were verified experimentally.

The load is applied to the inner frame (2) by means of the screw jack (12) which bears down on the load cell (13). This load is transmitted through a ball (14) which is carefully centred on the load cell, thereby eliminating the possibility of any spurious signals on account of eccentricity of loading. The jack is rigidly fixed on the top of a very stiff framework (15) constructed of laboratory "Meccano" sections. The load cell is used in conjunction with a strain gauge bridge, which gives strain readings corresponding to values of applied load.

To ensure that no load acts on the specimen due to the dead weight of the inner frame, the supports (16) are used. Basically, each consists of a framework to which is attached two bearings (17). A chain is fixed at one end to the top of the inner frame at (18), and passes over the bearings. Weights (19) are used to balance the downward load exerted by the inner frame, the load cell, and the end blocks, on the specimen.

The downward displacement of the inner frame (1) is measured by the dial gauge (20). The displacement of the bar (5) in Fig. 4 is measured by the dial gauge (21). The end rotations of the specimen at each stage of the loading programme can be determined from the readings of the two dial gauges.

Single element metal-foil resistance gauges were attached to the specimens at the mid and quarter points, on both extremes of the vertical diameters at these points. In this way it was possible to record the extreme compressive and tensile strains at 3 cross sections, and since it was possible for specimens to buckle at positions other than their mid-points, a better estimate of the critical strains at the buckling position was obtained by using strain readings from the strain gauges nearest the buckle position.

Readings of changes in vertical and horizontal diameters were taken at positions adjacent to the strain gauges, by means of a micrometer, in order to establish the magnitude of the cross-sectional ovalisation of the specimens.

THE TEST SPECIMENS

Steel and aluminium alloy tubes with a nominal diameter of 25 mm were used in the experiments; the thicknesses of the tubes were such that the radius-thickness ratios were in the range of approx. 15–40. In this range, it could be expected that a fair amount of plastic deformation would take place before collapse. The ratio of the unsupported length to the radius of the tubes was about 24, so that the end conditions would be expected to have a negligible effect on sections of the specimens furthest from the ends.

In order to obtain a fairly wide range of radius-thickness ratios, a number of lengths of 25 mm dia. steel and aluminium tubing were procured and drawn down to thinner wall thicknesses. The drawing process resulted in material whose mechanical properties differed

from tube-to-tube: each specimen had unique tensile and compressive stress–strain relations. Uniaxial, tensile and compression tests were therefore carried out for each set of tubes. For the tensile tests, coupons were cut from the tubes, parallel to their generators, while short cylindrical sections of tube were used for the compression tests. The stress–strain curves obtained were approximated analytically by the method of Ramberg and Osgood[9] who suggested that rising stress–strain curves with a smooth "knee" be represented by the relation

$$\epsilon = \frac{\sigma}{E}\left[1+\frac{3}{7}\left(\frac{\sigma}{\sigma_R}\right)^{n-1}\right] \tag{1}$$

where the variables in (1) are defined in Fig. 5(a). Figures 5(b) and 5(c) show actual, typical stress–strain curves which were obtained for steel and aluminium specimens, while the geometrical and stress–strain properties of all the specimens are listed in Table 1.

The stress σ_R is defined as the stress at which $E_S = 0.7E$, where E_S is the Secant modulus; the exponent n is found from the expression for the Secant modulus, i.e.

$$\frac{E}{E_S} = \frac{\epsilon}{\sigma} = 1+\frac{3}{7}\left(\frac{\sigma}{\sigma_R}\right)^{n-1}. \tag{2}$$

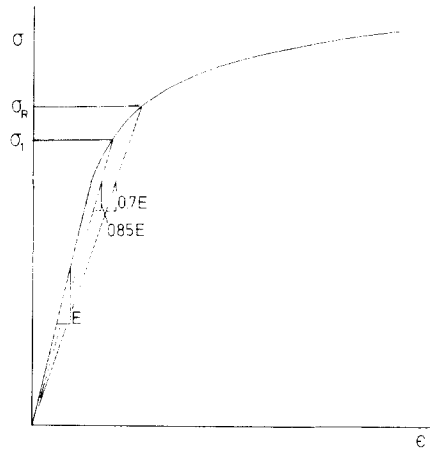

(a)

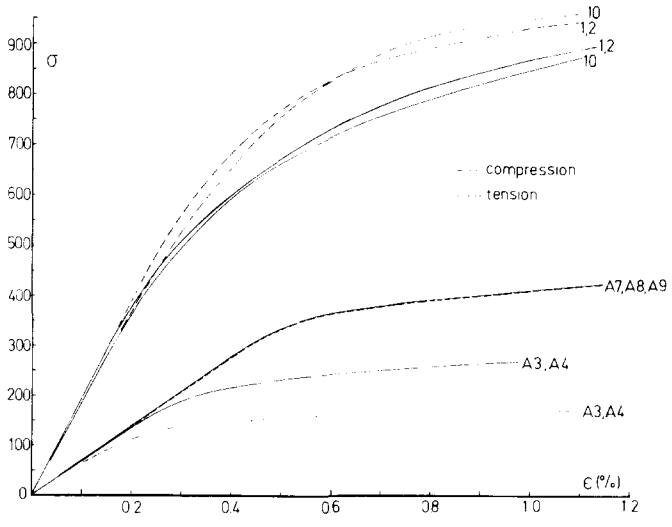

(b)

Fig. 5. (a) Definition of parameters in Ramberg–Osgood representation of stress–strain curves; (b) actual compressive and tensile stress–strain curves for specimens 1, 2, 10, A3, A4, A7, A8 and A9.

Table 1. Geometrical and material properties of specimens

Steel Specimens:

SPECIMEN	$\frac{r}{t}$	COMPRESSION σ_R/E	n	TENSION σ_R/E	n
1	38.25	0.0033	5.0	0.0042	6.8
2	38.90				
3	33.40	0.004	5.6	0.0040	4.6
4	30.73	0.0040	8.1	0.0046	6.3
5	25.67	0.0035	5.5	0.0045	6.9
6	25.71				
7	23.11				
8	23.14	0.0035	4.5	0.0043	3.9
9	23.14				
10	21.09	0.0039	5.9	0.0049	7.3

Aluminium Alloy Specimens:

SPECIMEN	$\frac{r}{t}$	COMPRESSION σ_R/E	n	TENSION σ_R/E	n
A1	27.71	0.00165	9.4	0.00242	15.8
A2	28.56				
A3	22.97	0.00329	9.1	0.00196	10.9
A4	23.05				
A5	18.46	0.00247	12.0	0.00280	21.6
A6	18.46				
A7	17.36				
A8	17.36	0.0057	15.3	0.0057	15.3
A9	17.36				

Evaluation of (2) at $E_S = 0.85\,E$ gives

$$n = \frac{\log_{10}(0.441)}{\log_{10}(\sigma_2/\sigma_R)} + 1 \tag{3}$$

where σ_2 is the stress at $E_S = 0.85\,E$.

TESTING PROCEDURE

The general test procedure involved the application of an increment of load through the screw jack and observations of the corresponding strains, changes in diameter and dial gauge readings. The load increments applied were such that an accurate picture of the moment-curvature relationships could be obtained.

Buckling of the test specimens always occurred suddenly and with a bang, partly on account of the comparative flexibility of the loading rig. (Even if the testing machine had been stiff, failure would probably have been sudden on account of the flexibility of the long pieces of tube on either side of the position of the buckle.) In order to obtain the load, strains, etc. as nearly as possible to the point of collapse, one of the strain readings was monitored continuously as the load was applied, so that its value would be known at collapse. The values of the other readings could than be found easily by extrapolation to the corresponding point. Since the strain increments were kept small, these extrapolated values would be a close estimate of the actual collapse values.

PRESENTATION OF RESULTS

Axial waves at buckling

Before we present the experimental values of moments, curvatures and strains, it is worthwhile to discuss an unexpected and important observation made during the tests.

Because of the highly polished surfaces of the tubes, it was possible to detect visually the presence of wave-like ripples on the compression sides of the specimens before collapse took place. These ripples were found to remain after unloading at the end of a test, and profiles of the ripples, taken along the extreme compression side, were obtained by use of a Taylor–Hobson Talylin 1 Straightness Measuring Instrument. The output from this scanning device is shown in Fig. 6 for some of the specimens. The wavelengths of the ripples were measured on the profiles, and the average values λ_{exp} are presented in Fig. 7, where they are made dimensionless with respect to the values of wavelength obtained by Batterman[8] in his analysis of the plastic axisymmetric buckling of axially compressed cylinders: these wavelengths are

$$\lambda_i = \frac{\pi\{rt(E/E_T + 3)\}^{1/2}}{\{3[(5-4\nu)E/E_T - (1-2\nu)^2]\}^{1/4}}, \tag{4a}$$

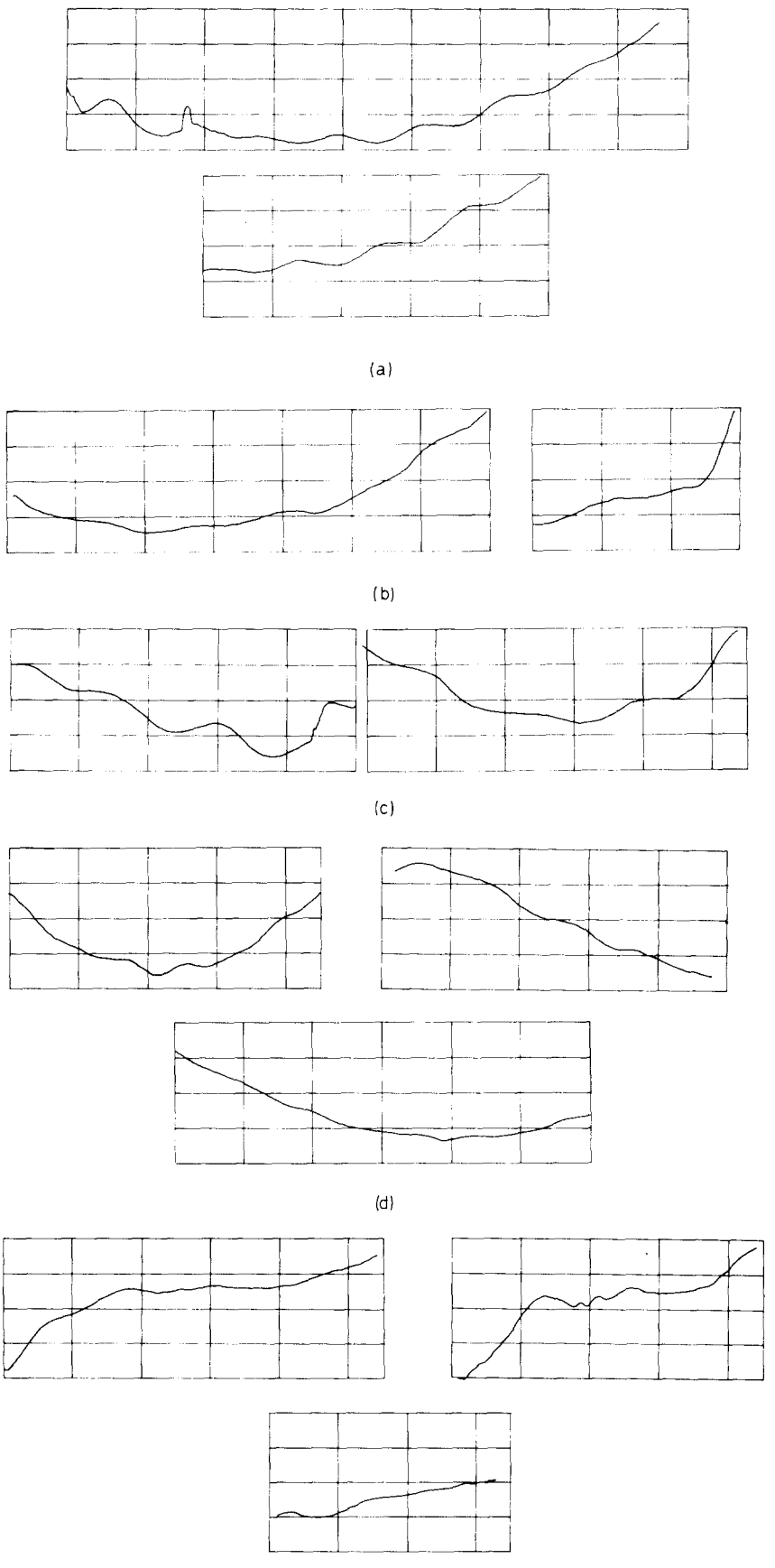

Fig. 6. Examples of longitudinal profiles for specimens 6(a), 8(b), 9(c), A2(d) and A6(e).

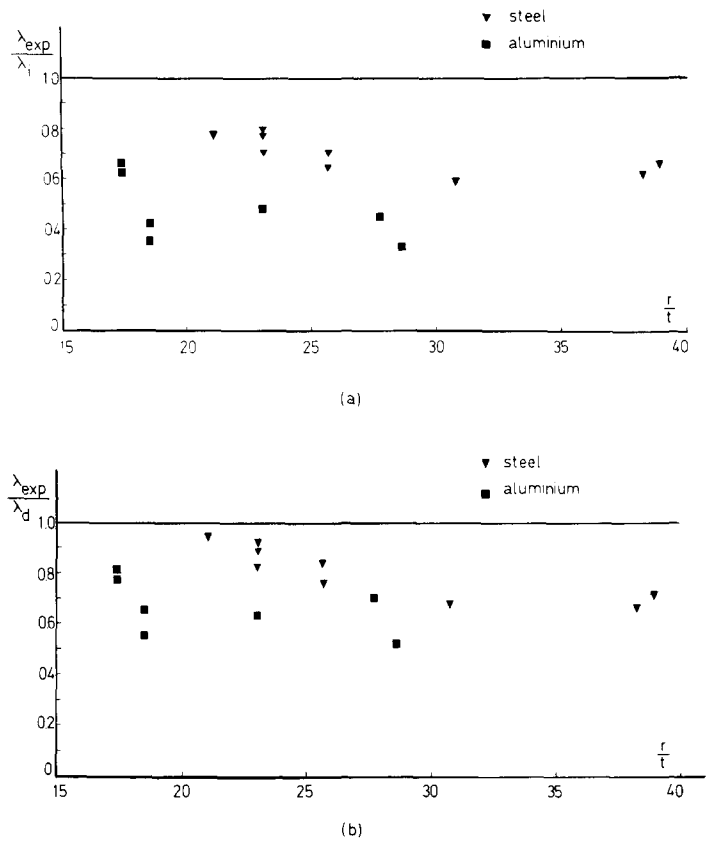

Fig. 7. Average experimental wavelengths vs r/t, and normalised with respect to: (a) λ_i (see eqn 4a); (b) λ_d (see eqn 4b).

$$\lambda_d = \frac{\pi\{rt(E/E_T + 3E/E_S)\}^{1/2}}{\{3[(3E/E_S + 2 - 4\nu)E/E_T - (1-2\nu)^2]\}^{1/4}} \tag{4b}$$

for J_2 flow theory and deformation theory, respectively; E_T and E_S are the tangent and secant moduli, respectively, of the stress–strain curve. The experimental values are closest to the values of λ_d for cylinders having the same radius-thickness ratios and compressive stress–strain properties, although in all cases less than the theoretical predictions. It is not clear why this is so, though there are several possible reasons: firstly, the fact that the ripples were first observed when the bending moment was about half the maximum value suggests the influence of imperfections. Another likely explanation for these discrepancies is that the wavelengths were measured when the tubes were in their final, collapsed state, whereas the theoretical values refer to wavelengths at buckling. Tests on axially compressed cylinders in the elastic range, using high-speed photography[10], have shown that initial modeforms and wavelengths are in good agreement with those obtained from an initial post-buckling analysis, while the final post-buckled mode shapes and wavelengths can be quite different.

Another possibility might be that the ripples are due to the propagation of end effects into the interior of the tube. This is unlikely, though, as the ripples were observed only over the interior of the tubes, i.e. in the region adjacent to where the tubes finally buckled. If these ripples were due to the propagation of end effects, they would than have been visible in regions adjacent to the ends as well, at some stage of the tests. The important point to be made here, though, is that these sine wave-type ripples suggest the presence of a mode of buckling deformation which is related to the axisymmetric buckling modes observed in axial compression tests on tubes buckling in the plastic range[8]. A comparison between critical strains for axially compressed tubes, and the maximum compressive values for the present set of tests, should throw further light on any connection between these two types of loading.

THE EFFECTS OF CHANGES IN DIAMETER

The changes in vertical and horizontal diameters of the specimens were measured at three positions along the length of the specimens at each stage of the loading programme, and the values which were recorded at the point nearest the position where buckling occurred were taken as a measure of the actual changes in diameter at this position. In all cases, the vertical diameter decreased and the horizontal diameter increased as the curvature increased. Buckling occurred in most cases in the middle third of the specimens: Fig. 8 shows one of the specimens in the final collapsed state. Experimental values of z(= change in diameter/original diameter) vs dimension-less curvature k ($= \kappa r^2 t$) are plotted in Fig. 9 for some of the specimens. Also shown is Brazier's[2] theoretical curve for cylindrical shells which buckle solely due to cross-sectional ovalisation.

In no case was the maximum change in diameter more than about 5% of the original diameter when collapse occurred. Also, the absolute changes in vertical and horizontal diameter were quite close to each other, indicating that the cross sections deformed into a near-oval cross-sectional shape. The relatively small changes in diameter which were recorded at the point of collapse are further suggestions that buckling was largely due to the growth of ripples.

We see also in Fig. 9 that, except in the initial stages of the tests, the experimental points lie on a straight line roughly parallel to Brazier's line, the equation for which is

$$z = 0.91\, k^2 \tag{5}$$

for a value of Poisson's ratio of 0.3. This suggests that a similar power-law relationdhip exists in the plastic case.

CRITICAL COMPRESSIVE STRAINS

The critical compressive strains are plotted against nominal radius-thickness ratio in Fig. 2, together with results obtained by Bouwkamp and Stephen[5], and by Wilhoit and Mervin[6] for cylindrical tubes in bending as well as results obtained by Batterman[8] from tests on aluminium tubes in axial compression. Also shown is the classical elastic line for cylinders in axial compression or in pure bending (to first order), the critical strain for which is ([3, 4])

$$\epsilon_{ce} = 0.6\, r/t \tag{6}$$

for a value of Poisson's ratio of 0.3. The points all lie within a well-defined band, with the strains for the steel specimens being generally higher. Furthermore, the points for our tests on

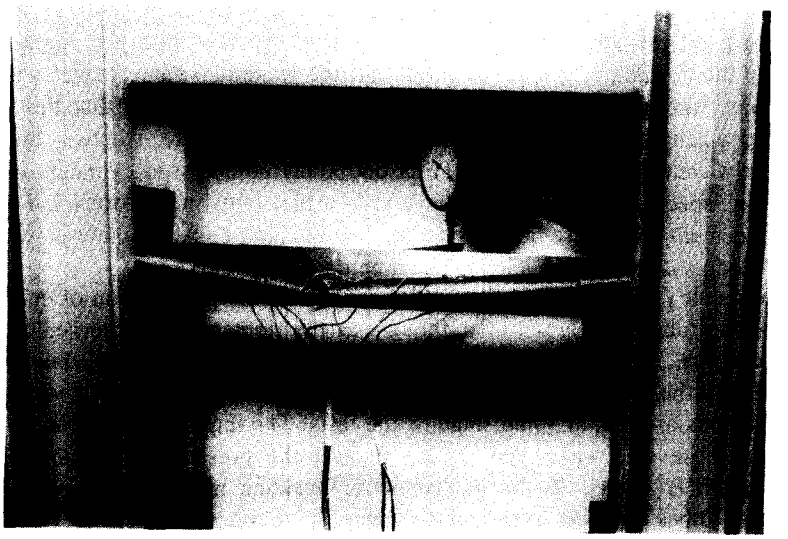

Fig. 8. Specimen 7 in the final collapsed state.

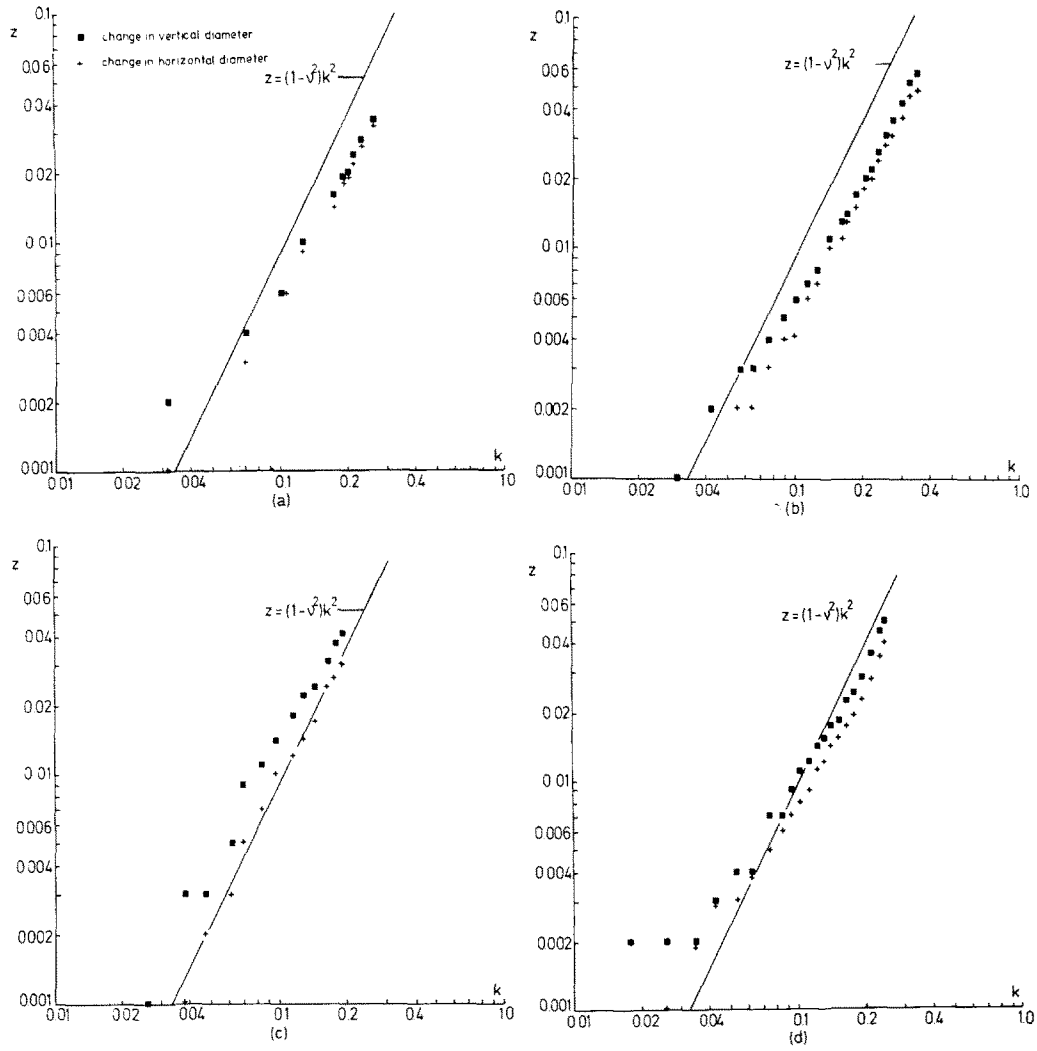

Fig. 9. Experimental values of z vs dimensionless curvature k for specimen 3(a), 5(b), A2(c) and A5(d).

aluminium specimens, and those of Batterman, show a similar relationship to radius-thickness ratio: this also applies to the points for our steel tests, when compared to those of Refs. [5] and [6]. With this similarity between results of cylinders tested under pure bending and axial compression in mind, the critical strains for the present set of tests were compared with the theoretical predictions of Batterman [8] for axially compressed tubes. Figures 10(a) and 10(b) show the experimental strains plotted vs r/t, where they are normalised with respect to Batterman's [8] theoretical values for J_2 flow theory and J_2 deformation theory, ϵ_{ci} and ϵ_{cd}, respectively: these are found from Batterman's formulae for incremental and deformation theory critical stresses,

$$\frac{\sigma_{ci}}{E} = \frac{2t}{r}\{3[(5-4\nu)E/E_T - (1-2\nu)^2]\}^{-1/2} \tag{7a}$$

$$\frac{\sigma_{cd}}{E} = \frac{2t}{r}\{3[(3E/E_s + 2 - 4\nu)E/E_T - (1-2\nu)^2]\}^{-1/2} \tag{7b}$$

and the uniaxial stress–strain curves (Table 1 and eqn 1). Both graphs show a great amount of scatter of the points, but the deformation theory predictions of critical strains are seen to be generally very much closer than those using flow theory. This discrepancy between the predictions of flow and deformation theories is one which has been shown to occur in many

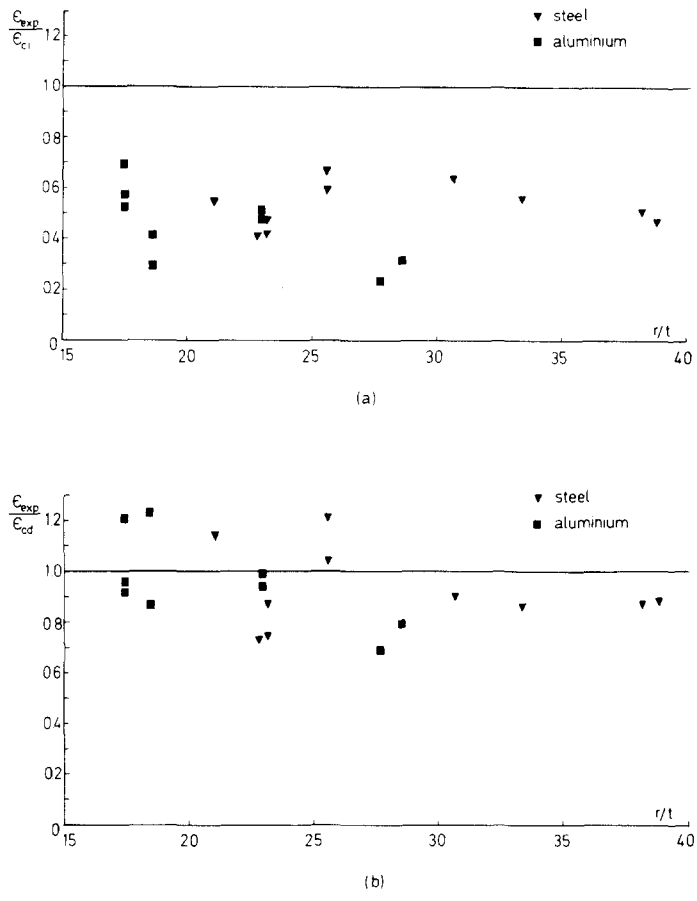

Fig. 10. Experimental critical strains vs r/t, and normalised with respect to: (a) ϵ_{ci} (see eqn 7a); (b) ϵ_{cd} (see eqn 7b).

different types of loading situations, with deformation theory results generally giving better agreement[11] with experiments.

We know that classical elastic buckling analyses of cylinders in pure bending give values of maximum compressive stress very close to those for axially compressed cylinders[3, 4]. Suer *et al.*[12] have summarised a number of experimental data for elastic cylinders in bending. These results show very clearly the imperfection-sensitivity for this type of loading in the elastic range.

In the plastic range, Batterman[8] has shown that cylinders in axial compression generally buckle in an axisymmetric mode, and not the diamond-shaped mode which is characteristic of elastic buckling. Furthermore, his experimental values of critical stress compare very well with theoretical values based on either flow or deformation theories, for radius-thickness ratios less that 60, with deformation theory results providing slightly better correlation.

Returning to the results in this paper, we see from Fig. 10(b) that the experimental strains lie in the range of 70–125% of the deformation theory strains for axial compression. In terms of *stresses*, this discrepancy is markedly less, since a fairly large difference in strain on the stress–strain curve corresponds to a much smaller difference in stress. This can easily be seen from the following calculations: for specimen A1, $\epsilon_{exp}/\epsilon_{cd}$ has a value of 0.69. The actual experimental strain is 0.00685, which corresponds to a value of experimental stress σ_{exp}, of 0.00203, using the stress–strain properties in Table 1. The value of σ_{cd}, corresponding to a value of theoretical strain ϵ_{cd} of 0.00993, is 0.00213. This gives a ratio of experimental stress to deformation theory stress of

$$\sigma_{exp}/\sigma_{cd} = 0.953.$$

A similar calculation for specimen 5, for which

$$\epsilon_{exp}/\epsilon_{cd} = 1.21, \text{ gives } \sigma_{exp}/\sigma_{cd} = 1.047.$$

Batterman's values of $\epsilon_{exp}/\epsilon_{cd}$ range from about 0.8 to 1.2 and σ_{exp}/σ_{cd} from 0.99 to 1.02.

It is clear that if we compare experimental and theoretical *stresses*, it will be found that the results are in very good agreement. But it is more satisfactory here, as outlined in the Introduction, to use *strain* as a buckling criterion, since the comparison of experimental with theoretical strain provides a much clearer idea of the amount of scatter of results. Also, from a practical point of view, it is far easier to estimate the local radius of curvature, and hence the strain, of a pipe from purely geometrical considerations.

The results given here may be useful in that they show a very definite range in which experimental strains are likely to lie when compared with deformation theory strains for axially compressed cylinders. Naturally, much more experimental data of this kind are necessary before a lower bound to the value of $\epsilon_{exp}/\epsilon_{cd}$ can be used with absolute confidence in a practical situation. What *can* be concluded, though, is that the experimental strains of cylinders in pure bending of a given material, are very similar to those for axial compression, for a given geometry, at least when the amount of ovalisation is small. This is borne out by Fig. 2.

MOMENT-CURVATURE RELATIONS

Dimensionless moment vs curvature graphs are shown in Fig. 11 for some of the specimens. The dimensionless moment m is defined by

$$m = M/Ert \tag{8}$$

while the dimensionless curvature k is given by

$$k = r/t. \tag{9}$$

The linear moment-curvature relation for an elastic thin-walled tube, from simple beam theory, is

$$M = EI\kappa = E\pi r^3 t\kappa \tag{10}$$

or

$$m = k. \tag{11}$$

Also shown in Fig. 11 are theoretical curves obtained from a beam-type analysis of an elastic–plastic cylinder in pure bending, which has the compressive and tensile properties of the specimen concerned, and with cross-sectional ovalisation not taken into account.

In most cases, the experimental curves in Fig. 11 fall below the theoretical curves. This is similar to the observations of Anderson[13], who tested a silicone rubber cylindrical tube in bending, and of Sherman[7], who carried out tests on mild steel tubes in bending. In the present case we can attribute this reduction in stiffness to the presence of the ripples before buckling ,

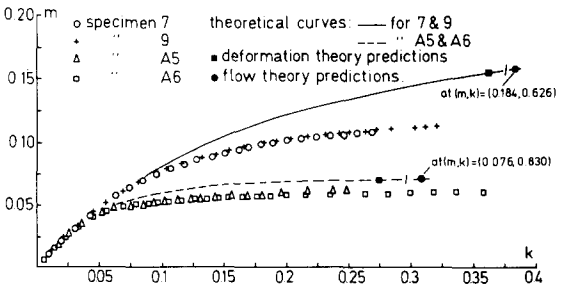

Fig. 11. Dimensionless moment-curvature relations for specimens 7, 9, A5 and A6, and corresponding theoretical curves.

as well as the slight amount of ovalisation which took place. It is also likely that an initial out-of-roundness contributed to the reduction in stiffness of the tubes, though the greatest amount measured before testing was only about 0.2% of the diameter.

It was found in general that the experimental moment-curvature curves were still rising when the collapse load was reached. This further emphasises the role played by the axial wave-type mode of deformation, particularly if we bear in mind that the nonlinearity of the stress–strain curves has a destabilising effect which would certainly enhance the onset of limit-point buckling due to excessive ovalisation, if this were to occur.

Theoretical approximations of critical moment-curvature are marked on the theoretical curves. These critical points were found by assuming that buckling occurred when the maximum compressive stress was equal to that given by [8] for tubes in axial compression. As we should expect, the points corresponding to deformation theory buckling stress are the closest approximation to the experimental maximum values.

CONCLUDING REMARKS

A series of tests have been made on aluminium and steel tubes which buckle in the plastic range, under pure bending. We have used as a buckling criterion the extreme fibre compression strain, rather than stress, since strain or curvature are easier to estimate in a practical situation. Also, the use of strain has given a clear idea of the amount of scatter of the data: a similar approach using stresses would show very little of this scatter.

Our investigation of the observed modes of deformation have led us to the conslusion that the ripples, rather than the small amount of ovalisation, were the primary cause of collapse in our tests. Further, the sine-wave nature of these ripples has led to the hypothesis that our tubes behaved as imperfect cylinders, the imperfections in which gave rise to a steady growth of these ripples which eventually lead to collapse.

The comparison of our critical strains with those obtained by others, has shown that the strains of our aluminium specimens and those of Batterman[8], who tested aluminium tubes in axial compression, have a similar relationship to radius-thickness ratio. This also applies to the results of our steel tests, when compared with those of Refs.[5] and [6].

We have also compared our experimental strains with the strains found from buckling analyses of perfect, axially compressed cylinders. The experimental strains are much closer to the J_2 deformation theory strains than those found from J_2 flow theory. In particular, the experimental strains lie within $\pm 30\%$ of the J_2 deformation theory strains; this corresponds to a range of about $\pm 5\%$ for corresponding stresses.† More experimental data of the kind we have presented are necessary before it can be stated with absolute certainty that a value of strain (and hence of local curvature) of about 70% of the J_2 deformation theory strain for an axially compressed cylinder, is a safe lower-bound, at least for plastic tubes which have very little ovalisation before buckling.

Acknowledgements—The author is very grateful to Mr. C. R. Calladine for his aid and advice throughout the entire investigation, and for his guidance in the preparation of this paper: to Dr. A. C. Palmer, for his inspiring ideas early on in the investigation: and to Dr. P. G. Lowe, for many helpful comments in the interpretation of the experimental results.

REFERENCES

1. A. C. Palmer, Personal communication.
2. L. G. Brazier, *Proc. R. Soc. Lon.* **A116**, 104–114 (1927).
3. P. Seide and V. I. Weingarten, *J. Appl. Mech.* **28**, 112–116 (1961).
4. B. D. Reddy and C. R. Calladine, *Int. J. Mech. Sci.*, **20**, 641–650, (1978).
5. J. G. Bouwkamp and R. M. Stephen, *J. Trans. Div. Am. Soc. Civ. Engrs* **99**, 521–536 (1973).
6. J. C. Wilhoit and J. E. Merwin, 5th Ann. Offshore Tech. Conf. Houston, 1973, paper, OTC. 1874.
7. D. R. Sherman, *J. Struct. Div. Am. Soc. Civ. Engrs* **102**, ST11, 2181–2195 (1976).
8. S. C. Batterman, *AIAA J.* **3**, 316–325 (1965).

†The author has very recently seen a thesis by Dr. S. Gellin[14], in which it is shown that the theoretical critical outer fibre strain of a cylinder in pure bending is practically equal to the critical strain of the same cylinder in axial compression, if deformation theory is used. The author is indebted to Prof. J. W. Hutchinson of Harvard University, for bringing to his attention Dr. Gellin's thesis.

9. W. Ramberg and W. R. Osgood, *NACA Tech.* Note No. 902, (1943).
10. R. C. Tennyson, *AIAA J.* **7**, 1481–1487 (1969).
11. J. W. Hutchinson, *Adv. Appl. Mech.* **14**, 67–144 (1974).
12. R. J. Anderson, Part II Report, Engineering Department, Cambridge University, 1975.
13. S. H. Suer, L. A. Harris, W. T. Skene and R. J. Benjamin, *J. Aero. Sci.* **25**, 281–287 (1958).
14. S. Gellin, Ph. D. Thesis, Harvard University (Nov. 1976).